

# Effect of mixed support of carbon black and nanographite on the activity of Pt catalyst for ethanol oxidation

Yuanyuan Chu · Zhaohui Teng · Bing Wu ·  
Yawen Tang · Tianhong Lu · Ying Gao

Received: 17 October 2007 / Revised: 2 April 2008 / Accepted: 16 April 2008 / Published online: 29 April 2008  
© Springer Science+Business Media B.V. 2008

**Abstract** The effect of the mixed support of carbon black and nanographite (CG) on the electrocatalytic activity and stability of the CG supported Pt (Pt/CG) catalyst for ethanol oxidation was investigated. It was found that the electrocatalytic activity and stability of the Pt/CG catalyst for ethanol oxidation depend on the weight ratio of carbon black and nanographite because the carbon black has a large surface area and nanographite has high conductivity. The Pt/CG catalyst with a weight ratio of 10:1 produces the best electrocatalytic activity and stability of the Pt/CG catalyst for ethanol oxidation.

**Keywords** Ethanol · Support · Carbon black · Nanographite · Pt

## 1 Introduction

Ethanol oxidation has been widely investigated because of its use in the direct ethanol fuel cell; this has various potential applications in transportation and portable electronic devices. Ethanol is a safe molecule and can be produced on a large scale from biomass. However, two major problems in DMFC are the low electrocatalytic activity and the stability of the catalysts for ethanol oxidation [1–4]. The catalysts for ethanol oxidation are usually Pt-based catalysts supported on porous carbon materials.

Several ways have been investigated to develop Pt-based binary catalysts for improving the electrocatalytic performance of Pt for ethanol oxidation. It is generally accepted that electrocatalytic performance is strongly dependent on the shape, size and distribution of the catalyst particles. On the other hand the particle size and distribution largely depend on the properties of the supports [5–6] once the preparation method and the components of the catalyst have been taken into account. Thus different supports for the Pt based catalysts, such as the carbon nanotubule [7], carbon nanofiber [8,9], carbon nanotube [10,11], macroporous carbon [12,13], graphitic carbon nanocoil [14,15] and ordered mesoporous carbon [16–22] have been investigated. The reason for using the carbon materials referred to above is because they possess large surface area and high electrical conductivity. However the prices of such carbon materials are high because of the harsh synthetic conditions and the low production yields. Considering that carbon black is a cheap carbon material with a very high surface area, but low electrical conductivity and that nanostructured graphite possesses high electrical conductivity, but low surface area, in this study we have used a mixture of carbon black and nanographite as support for the Pt catalyst. It was found that the mixed support enhances the electrocatalytic performance of the Pt catalyst for ethanol oxidation.

## 2 Experimental

### 2.1 Preparation of catalysts

The preparation procedure of the Pt/CG catalysts was as follows. After the mixture of carbon black (Vulcan XC-72R carbon black) and nanographite (Huatai Lubricant

Y. Chu · Z. Teng · B. Wu · Y. Gao (✉)  
Department of Chemistry, Harbin Normal University, Harbin  
150080, People's Republic of China  
e-mail: yinggao99@126.com

Y. Tang · T. Lu  
College of Chemistry and Environmental Science, Nanjing  
Normal University, Nanjing 210097, People's Republic of China

Sealing S&T CO. LTD) was agitated ultrasonically,  $\text{H}_2\text{PtCl}_6$  solution was added into the mixture at  $85^\circ\text{C}$ . Then formic acid solution was added drop by drop to reduce  $\text{H}_2\text{PtCl}_6$  at  $85^\circ\text{C}$  for 1 h. The suspension obtained was filtered and washed with triply distilled water until no  $\text{Cl}^-$  was detected. Finally the slurry was dried in vacuum at  $25^\circ\text{C}$  and the Pt/CG catalyst with 20 wt% Pt was obtained. The weight ratios of carbon black and nanographite in the Pt/CG catalysts were 1:1, 5:1, 10:1 and 15:1, respectively. The resultant Pt/CG catalysts are denoted as Pt/CG-1, Pt/CG-5, Pt/CG-10 and Pt/CG-15, respectively. The carbon black supported Pt catalyst prepared using a similar procedure to that mentioned above was designated as Pt/C.

## 2.2 Electrochemical measurements

The electrochemical measurements were carried out with a CHI650A electrochemical analyzer and a conventional three-electrode electrochemical cell. A Ag/AgCl electrode and the Pt foil were used as the reference and the counter electrode respectively. All potentials are quoted with respect to the Ag/AgCl electrode. The Pt/C and Pt/CG catalyst electrodes were used as the working electrodes. The preparation of the working electrode was as follows: an appropriate amount of the Pt/C or Pt/CG catalyst was mixed with the necessary amount of 5 wt% Nafion solution and 20 wt% PTFE. The mixture obtained was ultrasonically diluted in ethanol. Then the slurry was spread on carbon paper and dried at room temperature. The Pt loading for all the electrodes was  $1\text{ mg cm}^{-2}$ . The geometrical surface area of the working electrode was  $0.5\text{ cm}^2$ .

The electrochemical measurements were performed in a solution of  $1.0\text{ M C}_2\text{H}_5\text{OH} + 1.0\text{ M H}_2\text{SO}_4$  at  $25^\circ\text{C}$  or  $60^\circ\text{C}$ . Prior to the electrochemical measurements  $\text{N}_2$  was bubbled into the solution for 10 min to remove any dissolved  $\text{O}_2$ . During measurement,  $\text{N}_2$  was circulated above the solution. In order to measure the electrochemical specific surface area (ESA), with the electrode potential fixed at 0 V, CO was bubbled into  $0.5\text{ M H}_2\text{SO}_4$  solution at  $25^\circ\text{C}$  for 15 min until CO was fully adsorbed on the electrode.  $\text{N}_2$  was then bubbled into the solution for 10 min to remove CO. All the electrochemical measurements were carried out at  $25 \pm 1^\circ\text{C}$ . In the cyclic voltammetric measurements the scan rate was  $10\text{ mV s}^{-1}$ .

## 2.3 Physical characterization of the catalysts

X-ray diffraction (XRD) patterns of the catalysts were measured (Japanese D/max- $\beta\text{B}$ ) using a Cu K $\alpha$  source operating at 40 keV and 30 mA. Transmission electron microscopy (TEM) was performed with a Tecnais G2 Twins. Before the TEM examination the sample was firstly

ultrasonicated in ethanol for 20 min and then deposited onto 3 mm Cu grids covered with a continuous carbon film.

## 3 Results and discussion

### 3.1 Physicochemical characterization of catalysts

Figure 1 shows the XRD patterns of the Pt/C and Pt/CG catalysts. The peak at  $26.5^\circ$  in all the XRD patterns is characteristic of the (002) crystal face of the hexagonal structure of carbon. The peak is sharp, indicating that the CG support has a high content of graphite. In addition, in each XRD pattern, three characteristic peaks corresponding to Pt(111), (200) and (220) crystal faces of the face centered cubic crystalline of Pt are located at  $39.8^\circ$ ,  $46.2^\circ$  and  $67.5^\circ$ , respectively. The average size of the Pt particles in the Pt/C and Pt/CG catalysts can be calculated from the XRD patterns by means of the Scherrer equation [20].

$$d = \frac{0.9\lambda}{B_{2\theta} \cos \theta_{\max}} \quad (1)$$

where  $d$  is the average size of the Pt particles,  $\lambda$  is the wavelength of X-rays used ( $\lambda = 1.54056\text{ \AA}$ ),  $B_{(2\theta)}$  is the width at the half-maximum of the respective diffraction peak,  $\theta_{\max}$  is the angle at the position of the peak maximum. The Pt (220) diffraction peak was used here to calculate the average size of the Pt particles due to its low carbon interference in the XRD pattern. The average sizes

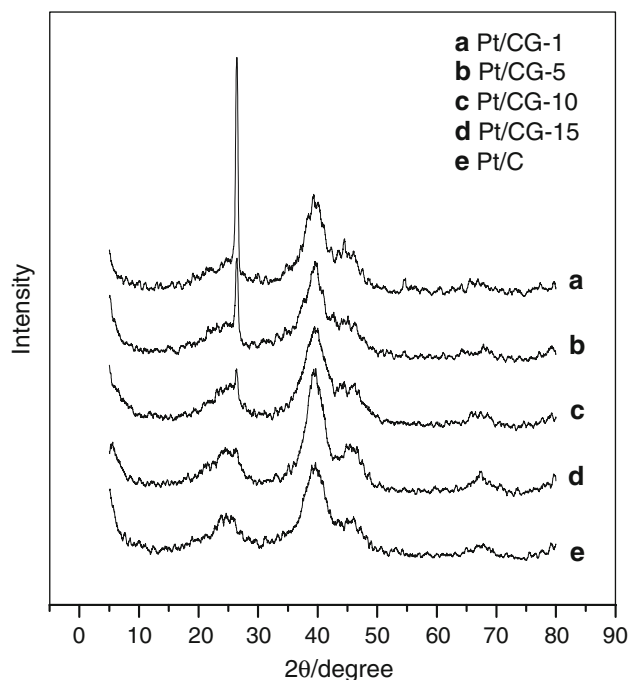


**Fig. 1** XRD patterns of (a) the Pt/CG-1, (b) Pt/CG-5, (c) Pt/CG-10, (d) Pt/CG-15 and (e) Pt/C catalysts

of the Pt particles obtained from the XRD patterns are listed in Table 1. The average sizes of the Pt particles in the Pt/C and the Pt/CG catalysts are in the range 2.7–3.4 nm, indicating that the supports slightly affect the average particle size.

Figure 2 displays the cyclic voltammograms of CO adsorbed on the different catalyst electrodes in 0.5 M H<sub>2</sub>SO<sub>4</sub> solution. ESA of the different catalyst electrodes can be calculated from Fig. 2 according to the following equation:

$$S = \frac{Q/k}{W \cdot L} \quad (\text{m}^2 \text{g}^{-1}) \quad (2)$$

where  $S$  represents ESA ( $\text{m}^2 \text{g}^{-1}$ ),  $W$  is the weight of catalyst (g),  $L$  is the weight percentage of Pt (wt%),  $Q$  is the no of C of the adsorption peak of CO (mC). The value of  $k$  is 4,200  $\text{mC m}^{-2}$ . The calculated ESA for the different catalysts are also listed in Table 1. It is clear that ESA is related to the average size of the Pt particles in the catalysts. The average size of the Pt particles in the Pt/CG-10 catalyst is the smallest among all the catalysts, 2.7 nm and thus, its ESA is the largest, 37.6  $\text{m}^2 \text{g}^{-1}$ .

Fig. 3a and b show TEM images of Pt/CG-10 and Pt/CG-15. The Pt particles of the two catalysts are highly dispersed

**Table 1** The particle sizes and ESA of the Pt/C and Pt/CG catalysts

Catalyst	Average size of Pt particles (nm)	ESA ( $\text{m}^2 \text{g}^{-1}$ )
Pt/CG-1	3.4	21.12
Pt/CG-5	2.8	33.0
Pt/CG-10	2.7	37.6
Pt/CG-15	2.8	34.4
Pt/C	2.9	32.6

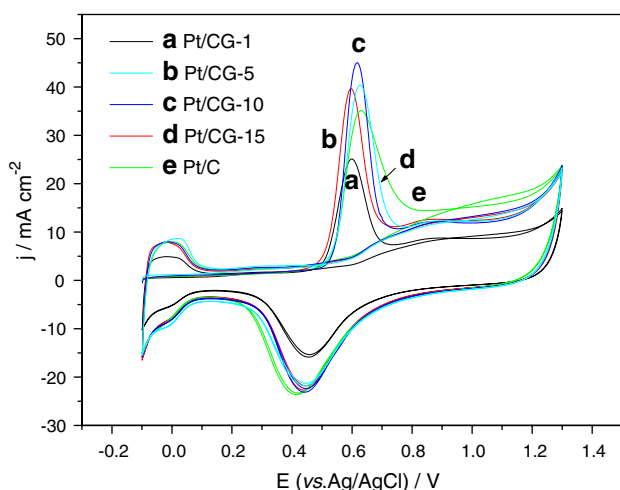


**Fig. 2** Cyclic voltammograms of CO adsorbed on (a) the Pt/CG-1, (b) Pt/CG-5, (c) Pt/CG-10, (d) Pt/CG-15 and (e) Pt/C catalysts electrodes in 0.5 M H<sub>2</sub>SO<sub>4</sub> solution at 25 °C. Scan rate: 10  $\text{mV s}^{-1}$

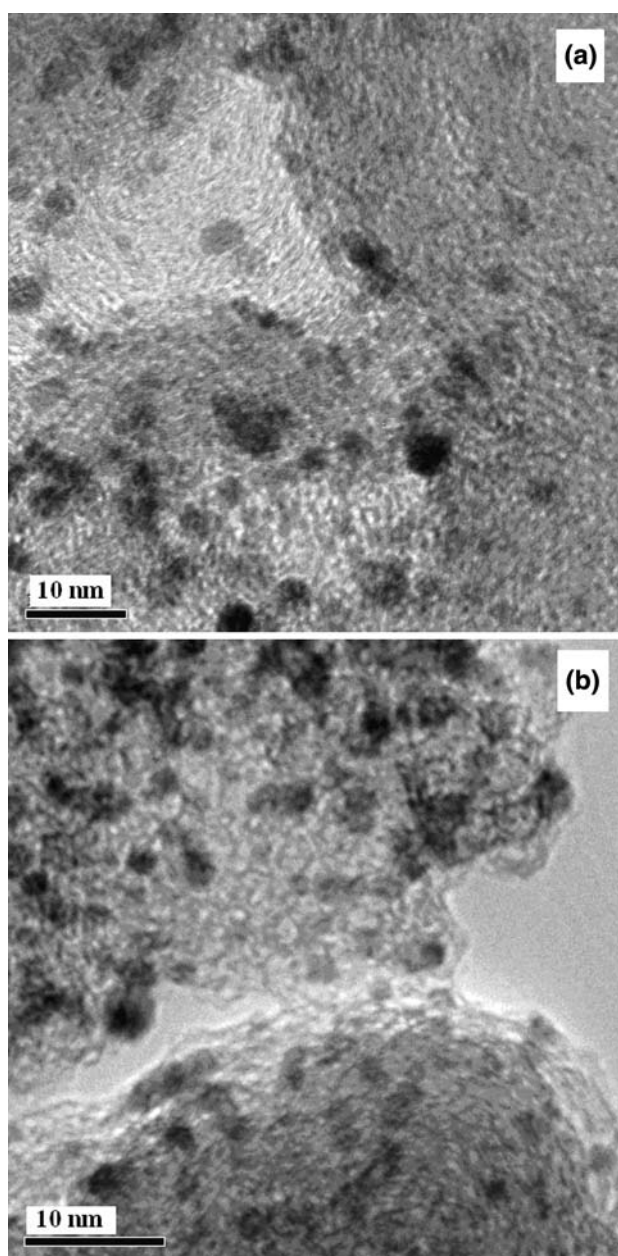
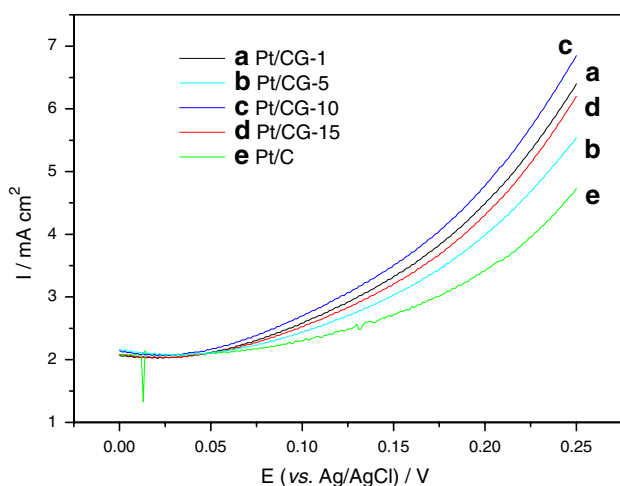


**Fig. 3** TEM images of (a) the Pt/CG-10 and (b) Pt/CG-15 catalysts and the average particle sizes are in good agreement with the calculated results from XRD measurement.

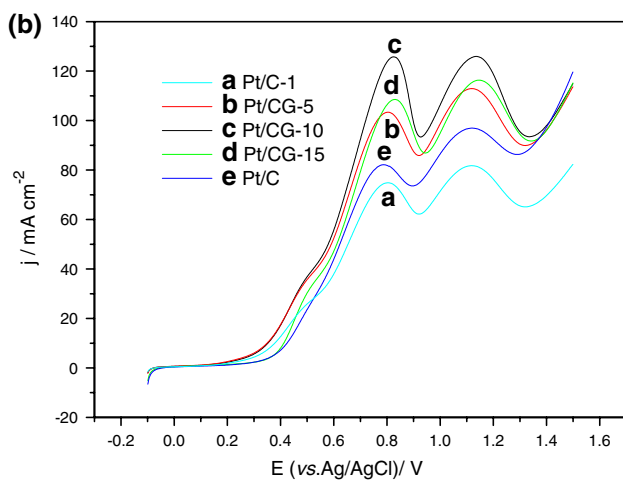
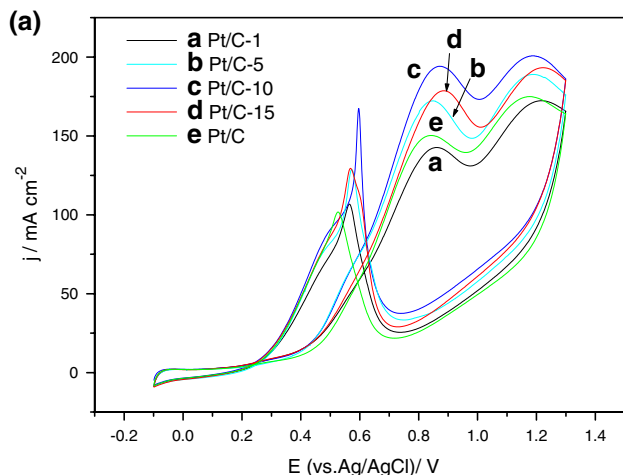
### 3.2 Electrocatalytic performance of different catalysts for ethanol oxidation

Figure 4 presents the linear sweep voltammograms of 1.0 M C<sub>2</sub>H<sub>5</sub>OH in 0.5 M H<sub>2</sub>SO<sub>4</sub> solution at the different catalyst electrodes at 25 °C. The onset potential of ethanol oxidation at the Pt/C catalyst electrode is more positive than that at all the Pt/CG electrodes.

Figure 5a shows the cyclic voltammograms of 1.0 M C<sub>2</sub>H<sub>5</sub>OH in 0.5 M H<sub>2</sub>SO<sub>4</sub> solution at the different electrodes



**Fig. 4** Linear sweep voltammograms of 1.0 M  $C_2H_5OH$  in 0.5 M  $H_2SO_4$  solution at (a) the Pt/CG-1, (b) Pt/CG-5, (c) Pt/CG-10, (d) Pt/CG-15 and (e) Pt/C catalysts electrodes at 25 °C. Scan rate: 10  $mV s^{-1}$



**Fig. 5** Cyclic voltammograms of 1.0 M  $C_2H_5OH$  in 0.5 M  $H_2SO_4$  solution at (a) the Pt/CG-1, (b) Pt/CG-5, (c) Pt/CG-10, (d) Pt/CG-15 and (e) Pt/C catalysts electrodes at 25 °C. (a) Scan rate: 10  $mV s^{-1}$  and (b) 2  $mV s^{-1}$

at 25 °C at 10  $mV s^{-1}$ . It is observed from Fig. 5a that, in the positive scan direction, there are two peaks at about 0.83 and 1.09 V for ethanol oxidation. The explanations for two peaks by other workers are not in good agreement. Fujiwara et al. [21] suggested that the peak at about 0.83 V is attributed to  $CO_2$  production and the peak at about 1.09 V is due to acetaldehyde formation. However Hitmi et al. [22] reported that ethanol is oxidized to acetaldehyde at about 0.83 V and to acetic acid at about 1.09 V. It was found that the potentials of two peaks for the different catalyst electrodes are similar. However the current densities of the peaks are different for the different catalyst electrodes. For example, current densities of the peak at about 0.83 V at the Pt/CG-1, Pt/CG-5, Pt/CG-10, Pt/CG-15 and Pt/C catalyst electrodes are 142.1, 171.7, 194.0, 178.2 and 149.9  $mA cm^{-2}$ . This indicates that initially the current density increases as the weight ratio of carbon black and nanographite in the catalysts decreases. When the weight ratio is 10:1 the current density reaches a maximum. Then the current density decreases with decreasing weight ratio. Thus the Pt/CG-10 catalyst showed the best electrocatalytic activity for ethanol oxidation.

Figure 5b shows the linear sweep voltammograms of 1.0 M  $C_2H_5OH$  in 0.5 M  $H_2SO_4$  solution at the different catalyst electrodes at 25 °C at 2  $mV s^{-1}$ . The peak current densities decreased and the peak potential is negatively shifted by about 50 mV when the scan rate is decreased to 2  $mV s^{-1}$ . However, the order of the current densities of two peaks at the different catalyst electrodes is the same as that for the scan rate of 10  $mV s^{-1}$  (Fig. 5a). The above results indicate that when the weight ratio is 10:1 the electrocatalytic activity of the Pt/CG catalyst is best because the carbon black possesses a large surface area and the nanographite has high conductivity.

Figure 6 displays the cyclic voltammograms of 1.0 M  $C_2H_5OH$  in 0.5 M  $H_2SO_4$  solution at the different catalyst

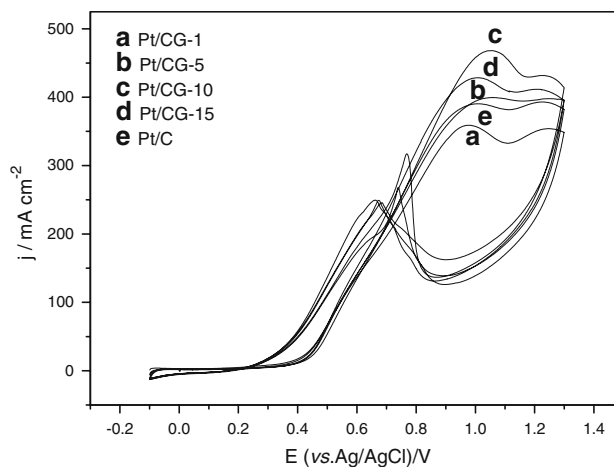
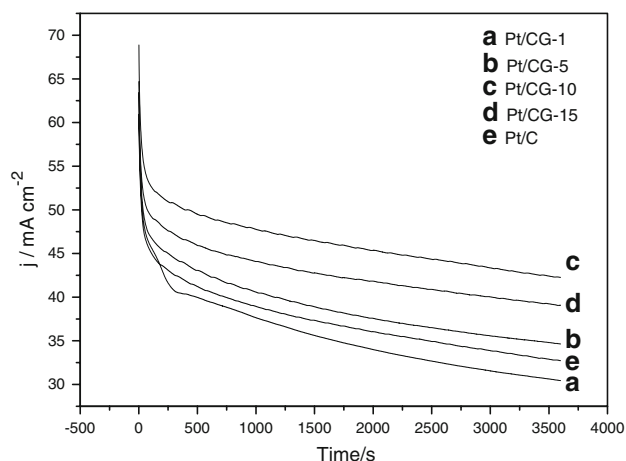


**Fig. 6** Cyclic voltammograms of 1.0 M  $C_2H_5OH$  in 0.5 M  $H_2SO_4$  solution at (a) the Pt/CG-1, (b) Pt/CG-5, (c) Pt/CG-10, (d) Pt/CG-15 and (e) Pt/C catalysts electrodes at 60 °C. Scan rate: 10  $mV s^{-1}$

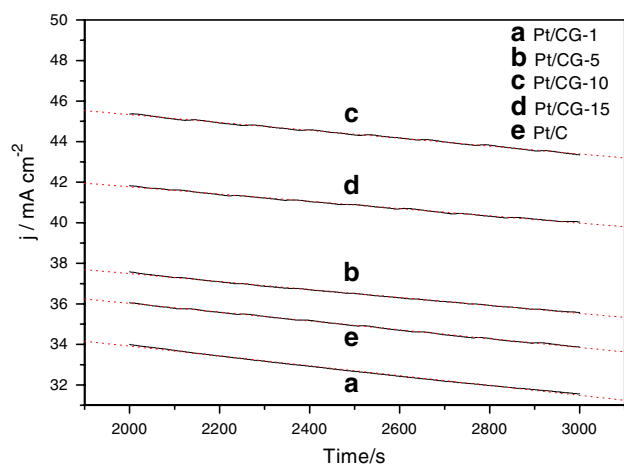
electrodes at 60 °C. At 60 °C, the Pt/CG-10 catalyst electrode also showed the best electrocatalytic activity for ethanol oxidation.

Figure 7 shows the chronoamperometric curves of 1.0 M C<sub>2</sub>H<sub>5</sub>OH in 0.5 M H<sub>2</sub>SO<sub>4</sub> solution at the different electrodes at 0.6 V and 25 °C. The current densities at Pt/CG-1, Pt/CG-5, Pt/CG-10, Pt/CG-15 and Pt/C at 3,600 s are 31.0, 36.0, 45.5, 42.0 and 33.5 mA cm<sup>-2</sup>, respectively. Thus the relationship between the electrocatalytic stability and the weight ratio is similar to that between the electrocatalytic activity and the weight ratio (Fig. 5 and 6). Pt/CG-10 shows the best electrocatalytic stability for ethanol oxidation.

Figure 8 shows the chronoamperometric curves of 1.0 M C<sub>2</sub>H<sub>5</sub>OH in 0.5 M H<sub>2</sub>SO<sub>4</sub> at 0.6 V and 25 °C in the



**Fig. 7** Chronoamperometric curves of 1.0 M C<sub>2</sub>H<sub>5</sub>OH in 0.5 M H<sub>2</sub>SO<sub>4</sub> solution at (a) the Pt/CG-1, (b) Pt/CG-5, (c) Pt/CG-10, (d) Pt/CG-15 and (e) Pt/C catalysts electrodes at 0.6 V and 25 °C



**Fig. 8** Chronoamperometry curves of 1.0 M C<sub>2</sub>H<sub>5</sub>OH in 0.5 M H<sub>2</sub>SO<sub>4</sub> solution at (a) the Pt/CG-1, (b) Pt/CG-5, (c) Pt/CG-10, (d) Pt/CG-15 and (e) Pt/C catalysts electrodes at 0.6 V and 25 °C in the range 2,000–3,000 s

region 2,000–3,000 s. The long-term poisoning rate ( $\delta$ ) can be calculated from Fig. 7 using the following equation [20]:

$$\delta = \frac{100}{I_0} \times \left( \frac{dI}{dt} \right)_{t > 500s} \quad (\% s^{-1}) \quad (3)$$

where  $(dI/dt)_{t > 500s}$  is the slope of the linear portion of the current decay and  $I_0$  is the current density at the start of polarization back extrapolated from the linear current decay. The  $\delta$  values and the current densities at 2,000 s calculated from Fig. 8 are listed in Table 2.  $\delta$  values of the different catalysts in the range 2,000–3,000 s follow the order Pt/CG-1 > Pt/C > Pt/CG-15 > Pt/CG-5 > Pt/CG-10 and the current densities at 2000 s showed the reverse order. This shows that the Pt/CG-10 catalyst possesses high poisoning tolerance.

Long time cycling of the Pt/CG-10 electrode is shown in Fig. 9. The current density increased slowly during the first 100 cycles. This also indicates good electrocatalytic stability of Pt/CG-10.

**Table 2** The  $\delta$  values and the current densities at 2,000 s of the different catalysts obtained from Fig. 8

Catalyst	$\delta / s^{-1} (\times 10^3)$	Current density at 2,000 s (mA cm <sup>-2</sup> )
Pt/CG-1	7.15	34.00
Pt/CG-5	5.22	37.58
Pt/CG-10	4.28	45.36
Pt/CG-15	4.30	41.84
Pt/C	6.05	36.06

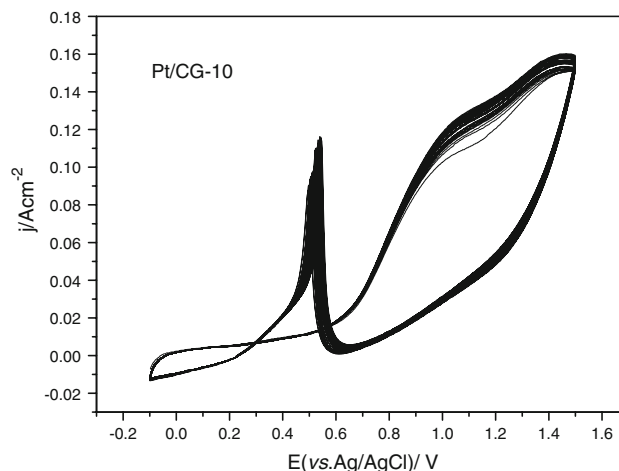


**Fig. 9** Cyclic voltammograms of 1.0 M C<sub>2</sub>H<sub>5</sub>OH in 0.5 M H<sub>2</sub>SO<sub>4</sub> solution at Pt/CG-10 catalyst electrodes for 100 cycles at 25 °C. Scan rate: 50 mV s<sup>-1</sup>

#### 4 Conclusion

The present work demonstrates that mixed support of carbon black and nanographite showed clear effects on the electrocatalytic activity and stability of Pt catalysts for ethanol oxidation. The electrocatalytic activity and stability of the Pt catalyst depends on the weight ratio of the mixed support of the carbon black and the nanographite. Initially the electrocatalytic activity and stability of the Pt catalyst for ethanol oxidation increases with decreasing weight ratio in the catalysts. When the weight ratio is 10:1 the highest electrocatalytic activity and stability are reached. If the weight ratio is further increased, the electrocatalytic activity and stability decrease. The results are related to the high surface area of carbon black and the high conductivity of nanographite.

**Acknowledgments** The authors are grateful for financial support by the State Key High Technology Research Program of China (863 Program, 2006AA05Z137, 2007AA05Z143), Nature Science Foundation of China (20573029, 20573057), Natural Science Foundation of Heilongjiang Province(B200505) of China, the Innovation fund for graduate students of Heilongjiang Province(YJSCX2007-0314HLJ), Fund of Department of Science and Technology of Jiangsu Province (BK2006224), the Natural Science Foundation of the Education Committee of Jiangsu Province (05KJB150061).

#### References

1. Song S, Tsiakaras P (2006) *Appl Catal B: Environ* 63:187
2. Sun F, Wu B, Qu W et al (2005) *Chin J Inorg Chem* 21:1546
3. Gupta SS, Datta J (2006) *J Electroanal Chem* 594:65
4. Lamy C, Rousseau S, Belgsir EM, Coutanceau C, Leger JM (2004), *Electrochim Acta* 49:3901
5. Dosanjios DM, Kokoh KB, Leger JM et al (2006) *J Appl Electrochem* 36:1391
6. Prabhuram J, Zhao TS, Liang ZX, Chen R (2007) *Electrochim Acta* 52:2649
7. Raghuvveer V, Manthiram A (2005) *J Electrochem Soc* 152:1504
8. Bagchi J, Bhattacharya SK (2007) *J Power Sources* 163:661
9. Wu G, Chen Y-S, Xu B-Q (2005) *Electrochem Commun* 7:1237
10. Treesukol P, Srisuk K, Limtrakul J et al (2005) *J Phys Chem B* 109(24):11940–11945
11. Baker RTK, Laubernds K, Wootsch A (2000) *J Catal* 193:165
12. Bessel CA, Laubernds K, Rodriguez N et al (2001) *J Phys Chem B* 105:1115
13. Steigerwalt ES, Deluga GA, Cliffel DE et al (2001) *J Phys Chem B* 105:8097
14. Chien CC, Jeng KT (2006) *Mater Chem Phys* 99:80
15. Joo SH, Choi SJ, Oh I et al (2001) *Nature* 412:169
16. Ryoo R, Joo S H, Jun S (1999) *J Phys Chem B*103:7743
17. Kwon S, Vidic R, Borguet E (2002) *Carbon* 40:2351
18. Che G, Lakshmi BB, Fisher ER, Martin CR (1998) *Nature* 393:346
19. Jiang J, Kucernak A (2003) *J Electroanal Chem* 543:187–199
20. Guo JW, Zhao TS, Prabhuram J et al (2005) *Electrochim Acta* 51:754
21. Fujiwara N, Friedrich KA, Stimming U (2001) *J Electroanal Chem* 500:518
22. Hitmi H, Belgsir EM, Leger J-M, Lamy C, Lenza RO (1994) *Electrochim Acta* 39:407